Role of finite boson number in the interacting boson approximation description of $\gamma \rightarrow g$ transitions in deformed nuclei

R. F. Casten and D. D. Warner
Brookhaven National Laboratory, Upton, New York 11973

A. Aprahamian
Clark University, Worcester, Massachusetts 01610

(Received 22 February 1983)

The effect of finite boson number in the interacting boson approximation is one of its most distinguishing features. These effects are investigated in terms of the deviations of $\gamma \rightarrow g$ band $E2$ transitions from the rotational (Alaga) values which provide one of the most crucial tests of collective models of deformed nuclei. It is shown that the empirical systematics of these deviations displays a strong mass dependence, that the interacting boson approximation successfully reproduces these systematic trends, and does so primarily by virtue of the variations in boson number and not because of parameter variations. Moreover, the origin of the N dependence lies in the characteristic way in which the SU(3) symmetry is broken in calculations for realistic deformed nuclei and involves, in an essential way, the N dependence of the SU(3) $\gamma \rightarrow \beta$ transitions.

[NUCLEAR STRUCTURE Interacting boson model, finite boson number effects, relation to geometric models.]

I. INTRODUCTION

The formalism[1-3] of the interacting boson approximation (IBA) incorporates an explicit dependence on boson number N, where N is the sum of the number of s and d bosons ($N = n_s + n_d$) and, in this feature, differs essentially from geometrical or shape models. Nevertheless, recent studies have indicated that the two approaches become largely equivalent as $N \rightarrow \infty$. Thus, there has long been active interest both in the relation between this model and geometrical models and in the role played by finite N in the predictions of the IBA. These issues are of broader importance because of the light they may shed on the more general question[4] of the significance of levels from adjacent shells in the structure of low lying collective states in heavy nuclei.

For a number of years, it was thought that the effects of finite boson number in the IBA would show up most dramatically among high spin states in terms of spin cutoffs at $I = 2N$ and falloffs toward zero in $B(E2)$ values connecting successive high spin states of, for example, the quasiground band. A number of experimental tests[5-7] were indeed carried out, with mixed results, but it has recently become recognized that it is in just such states that one approaches the limit of expected applicability of the IBA in that other degrees of freedom, such as two particle pair excitations, begin to play a major role.

Conversely, for low spin states, it was then widely anticipated that finite N effects would be of little *practical* importance. For example, in the SU(5) limit, the IBA predicts a $B(E2)$ value from the two phonon to one phonon state that is related to the one phonon to ground state $B(E2)$ value by the factor $2(N-1)/N$, which goes to the geometrical limit of 2 as $N \rightarrow \infty$. For typical vibrational nuclei, where $N \approx 6$—8, this correction is only $\approx 15\%$. In deformed nuclei, where $N \approx 12$—18, one might expect such finite N effects to be even smaller.

However, very recently, some results have begun to emerge[8-10] for deformed nuclei that suggest that these effects *are* extremely important for low lying low spin states. Indeed, finite N effects are the key ingredient in enabling the IBA to generate systematic predictions over series of nuclei that are borne out empirically. It is the purpose of this paper to address the question of the role of finite N in the IBA by examining $\gamma \rightarrow g$ band $E2$ transitions in deformed nuclei which, as will be evident below, are a particularly sensitive probe of these effects. Moreover, it will be shown that a study of the origin of these N effects provides an explanation for their unexpected importance.

II. FINITE BOSON NUMBER EFFECTS IN DEFORMED NUCLEI

A. General discussion

In this paper the discussion is limited to deformed, or near deformed, nuclei where the γ band is below the β band. The reason for this restriction is practical, not fundamental, namely, that the IBA Hamiltonian that can be used to describe these nuclei is particularly simple: The essential predictions in fact depend on a single parameter.

The IBA Hamiltonian of relevance here, then, is simply[8]

$$H = -\kappa Q \cdot Q - \kappa' L \cdot L \ , \tag{1}$$

where

$$Q = (s^{\dagger}\tilde{d} + d^{\dagger}s)^{(2)} + \frac{\chi}{\sqrt{5}}(d^{\dagger}\tilde{d})^{(2)} \tag{2}$$

and L is the boson angular momentum operator. The operator Q also determines $E2$ transition rates since the

$E2$ operator is $T(E2)=\alpha Q$. The coefficient χ in Q is taken as a free parameter which is allowed to vary from the SU(3) value of $-\sqrt{35}/2=-2.958$ down to the O(6) value of zero. Since χ also determines the relative strengths of $E2$ transitions, it is usually fixed from a ratio of $B(E2)$ values, a suitable one being the ratio

$$B(E2;2_\gamma\rightarrow 0_g)/B(E2;2_g\rightarrow 0_g) .$$

This ratio has an inter-band, inter-representation transition in the numerator and is therefore zero in the SU(3) limit: For $\chi\neq -2.958$, it is finite and highly sensitive to χ. The other parameters in H and $T(E2)$ are of no consequence whatsoever for the present discussion. The constant α is merely an overall normalization factor for $B(E2)$ values. The $L\cdot L$ term is diagonal and therefore cannot change the energy separation of states of the same spin nor their wave functions. The parameter κ also has no effect on wave functions or transition rates. It serves only to determine the overall energy scale. Thus, the model, as used here, involves a one parameter calculation. Of course, it is not intended that H of Eq. (1) will be sufficient to adequately describe each deformed nucleus in detail. Certainly, additional terms, such as one in $\kappa'' P\cdot P$, may have to be added to fine tune the predictions. Such refinements, however important in actual calculations, are extraneous to the present discussion and may be ignored.

One of the most interesting predictions of the IBA, and one that will be shown to play an important role in the structure and N dependence of $\gamma\rightarrow g$ transitions, is that of strong, allowed $E2$ transitions connecting β and γ bands in deformed nuclei. These transitions are a feature in direct opposition to the pure harmonic geometric model in which such transitions are forbidden since they would change the phonon number by two. They arise in the IBA as a natural consequence of the SU(3) limit and, indeed, persist in calculations with broken SU(3) for typical deformed nuclei where they continue to dominate the $\beta\rightarrow g$ transitions. These transitions are difficult to detect empirically due to their low energy but have been observed[11–13] and do indeed dominate $\beta\rightarrow g$ transitions where the appropriate experiments have been carried out.

B. γ-g band mixing

The IBA in deformed nuclei has been shown[8,14,15] to successfully account for the detailed branching ratios of $\gamma\rightarrow g$ transitions and to include "automatically" the observed empirical deviations of these branching ratios from the simple rotational (Alaga) values.

It is perhaps easiest to discuss this feature in the context of the Mikhailov plot formalism. This has been described elsewhere.[14–16] The essential point is that, in the presence of $\Delta K=2$ mixing, the $\gamma\rightarrow g$ $B(E2)$ values are modified and, under certain approximations, can be expressed by

$$\left[\frac{B(E2;I_\gamma\rightarrow I_g)}{2\langle I_\gamma 22-2\,|\,I_g 0\rangle}\right]^{1/2} = M_1 - M_2[I_g(I_g+1)-I_\gamma(I_\gamma+1)] , \quad (3)$$

where I_g is a ground band spin and I_γ is a γ band spin. The quantities M_1 and M_2 are directly related to the direct (unmixed) $\Delta K=2$ transition matrix element and the γ-g mixing amplitude, respectively. Explicitly,

$$M_1=\langle\psi_g||E2||\psi_\gamma\rangle-4M_2 ,$$
$$M_2=(15/8\pi)^{1/2}eQ_0\epsilon_\gamma . \quad (4)$$

Here, ϵ_γ is the spin independent part of the γ-g mixing amplitude. The full mixing amplitude is given by $\epsilon_\gamma f'_\gamma(I)$, where

$$f'_\gamma(I)=\sqrt{2}[(I-1)I(I+1)(I+2)]^{1/2} .$$

The approximations inherent in Eq. (3) are that one can neglect other spin dependent $\Delta K=2$ mixing effects, that the quadrupole moments of the ground and γ bands are the same, and that the spin dependence of the mixing $f'_\gamma(I)$ is that arising from $\Delta K=2$ mixing of rotational wave functions. In typical deformed nuclei, all three assumptions are generally well satisfied insofar as their impact on $\gamma\rightarrow g$ transitions is concerned.

The advantage of Eq. (3) is that, essentially, the intrinsic $E2$ transition matrix elements on the left are described by a straight line with intercept M_1 and slope M_2 when plotted against $I_g(I_g+1)-I_\gamma(I_\gamma+1)$. Thus, via this formalism, any set of data, or calculations, which fall on a straight line on a Mikhailov plot, can be dissected to disclose separately the implicit direct transition matrix element contained in M_1 and the mixing effects given by M_2. The most common[8,14–16] indicator of the mixing is the parameter Z_γ which is given by

$$Z_\gamma=\frac{-2M_2}{M_1+4M_2} , \quad (5)$$

which can be deduced from branching ratios rather than absolute $B(E2)$ values.

Given that an IBA calculation correctly gives the direct average $\Delta K=2$ $\gamma\rightarrow g$ transition matrix element, which, in practice, is ensured by the choice of the parameter χ, and that both the data and the IBA calculations lie on a straight line on a Mikhailov plot, then the extent of agreement or disagreement between the data and calculations for *all* the $\gamma\rightarrow g$ transitions can be compactly assessed by extracting and comparing empirical and predicted effective values of the single parameter Z_γ. In Ref. 8, such a comparison was presented for a number of nuclei in the rare earth region. The empirical Z_γ values showed a rather smooth behavior for each element and the IBA calculations agreed with the data within a factor of 2 in all cases.

In order to investigate this more thoroughly, a more extensive literature search has been instituted to obtain a larger number of empirical Z_γ values, particularly in the upper half of the rare earth region (Yb, Hf, W, and Os nuclei). In most cases it has been possible to extract these values from a full multipoint Mikhailov analysis: In a few cases only one or a pair of branching ratios was known. The search covered all deformed and transitional nuclei[11,13,17–41] subject to the criterion that $E_\gamma<E_\beta$. The empirical systematics of Z_γ values, shown in Fig. 1, display a remarkable behavior when plotted against a boson number. The values exhibit a smooth cup-shaped systematics with a minimum at midshell. This regularity in itself suggests a simple underlying mechanism and strongly hints that the mechanism is related to the variations in

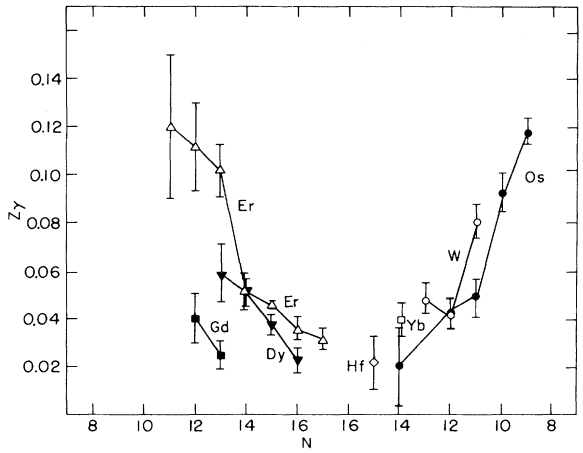

FIG. 1. Systematics of empirical Z_γ values extracted from $B(E2)$ ratios of Refs. 11, 13, and 17–41 for rare-earth, deformed nuclei with $E_\gamma < E_\beta$ plotted as a function of N.

the number of valence nucleons.

In order to compare these empirical Z_γ values with ones calculated with the IBA, the appropriate χ values must first be determined, using ratios of $\gamma \rightarrow g$ to $g \rightarrow g$ $B(E2)$ values. These have been extracted for the nuclei of Fig. 1 and the results are shown in Fig. 2. It is important to note that, for the nuclei in the center of the region displayed in Fig. 1 (the well deformed nuclei), the χ values fall in *a narrow range which can be conservatively encompassed by the values from -0.9 to -1.2.* For the transitional nuclei, such as the very neutron deficient Er isotopes and the heavy Os isotopes which, in each case, are approaching the O(6) limit, the χ values drop well below this range.

Recalling that the quantity Z_γ is only properly defined if a Mikhailov plot yields a straight line, it is necessary before proceeding further to verify that such a behavior is indeed characteristic of these IBA calculations. This is most easily done by presenting a matrix of Mikhailov

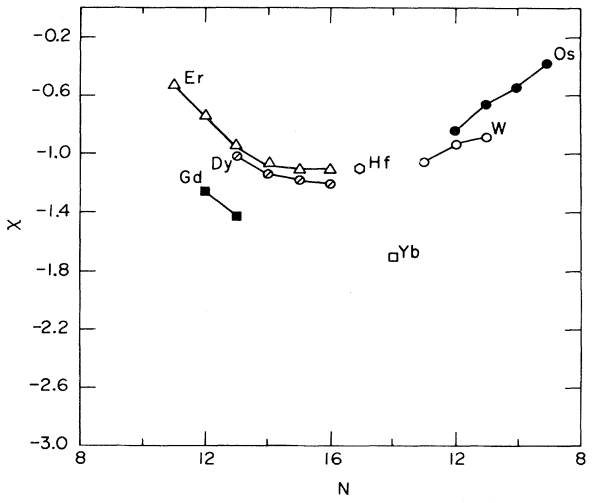

FIG. 2. Empirical χ values [see Eq. (2)] deduced for the nuclei in Fig. 1.

plots for a set of N and χ values. Figure 3 shows Mikhailov plots of IBA calculations of $\gamma \rightarrow g$ transitions for $N = 16$, 12, and 10 and $\chi = -1.5$, -1.0, and -0.5. It is clear from the figure that the IBA leads to a straight line for large N and $|\chi|$ values. As either decreases, a curvature begins to appear, most notably a rolling over for spin increasing transitions. Closer inspection shows that, if $|\chi| \cdot N > 12$, a reasonable straight line results.

In light of the above discussion and Fig. 3, it is evident that the calculated Z_γ values for the transitional light Er and heavy Os nuclei must be extracted from partially curved Mikhailov plots and thus are only of approximate validity and even then primarily so only for spin decreasing transitions. With this caveat in mind, the calculated Z_γ values can be compared with the empirical ones and the results are indicated by the dashed lines in Fig. 4. It is clear that, overall, the IBA reproduces the empirical values of Z_γ rather well both over the entire region as well as for each element. In all cases, the agreement is again within a factor of 2. The Z_γ values are underestimated for the very light Er nuclei, but the arguments given above imply that the Mikhailov-based comparison should be treated more qualitatively in such cases.

Since the IBA does reproduce the empirical Z_γ systematics which themselves exhibit an apparent boson number dependence, it remains for us to ascertain if this dependence arises in the IBA implicity, via changes in χ, or directly, via the boson number variations in the structure of the IBA states. As pointed out earlier, the χ values for most well deformed nuclei fall in a narrow range. The band of Z_γ values corresponding to this range is shown in Fig. 5. This provides a conservative way of distinguishing χ from N effects by utilizing the extreme values of χ for well deformed nuclei. It is clear from the figure that *the IBA automatically gives a cup-shaped variation of Z_γ by virtue of the explicit variation with mass of the boson number.*

Not only does this result highlight the importance of boson number effects in determining the predictions of the IBA, even for low lying, low spin states, but it also points to the underlying microscopy behind the IBA in the sense that, although the IBA is ostensibly phenomenological, it provides many predictions that are beyond the scope of geometrical models unless microscopic [e.g., random phase approximation (RPA)] ingredients are introduced externally.

The discussion so far has been mainly restricted to those nuclei for which $0.9 \leq |\chi| \leq 1.2$, and therefore excludes some of the larger Z_γ values in Fig. 1, corresponding to N and χ values where the Mikhailov plots for the IBA exhibited substantial curvature. However, one can still estimate *approximate* Z_γ values for these nuclei. The results were presented in Fig. 4 and, as remarked in the context of that figure, show reasonable agreement with the data. To understand the origin of the large Z_γ values for the transitional low N Er and Os nuclei, it is useful to present an expanded form of Fig. 5 where Z_γ contours for a larger range of χ values are included, and where the Z_γ value for each nucleus is indicated by positioning it according to its N and χ values. This is shown in Fig. 6. It is important to note that for the transitional nuclei, the boson number is no longer the controlling factor. Now, it is primarily the rapidly decreasing χ values (see Fig. 2), albeit reinforced

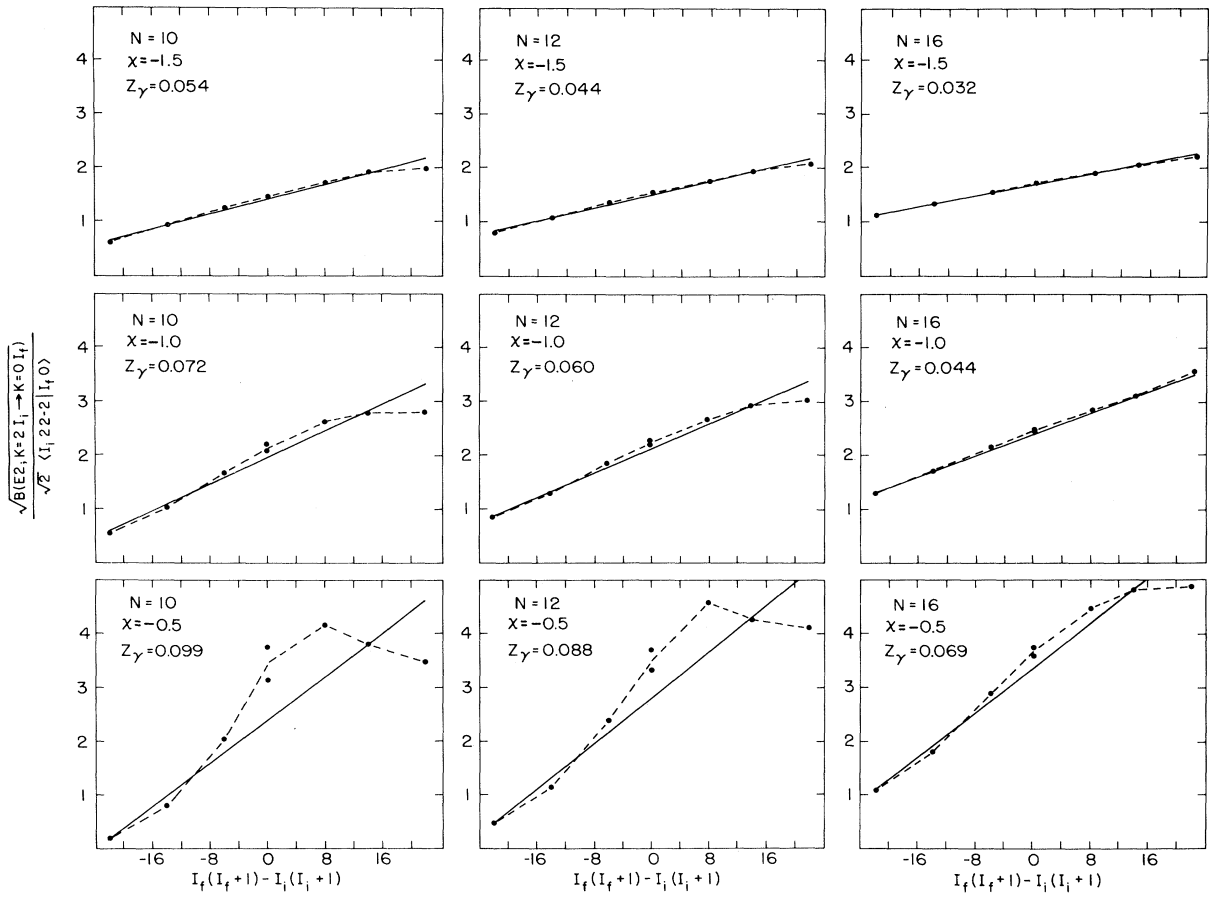

FIG. 3. Matrix of IBA ($\gamma \rightarrow g$ transition) Mikhailov plots for $N = 10$, 12, and 16 and $\chi = -1.5$, -1.0, and -0.5. The points are the IBA calculations. The dashed lines are drawn through these points to guide the eye. The solid lines are linear least squares fits to the plotted points and the Z_γ values correspond to the slopes of the solid lines.

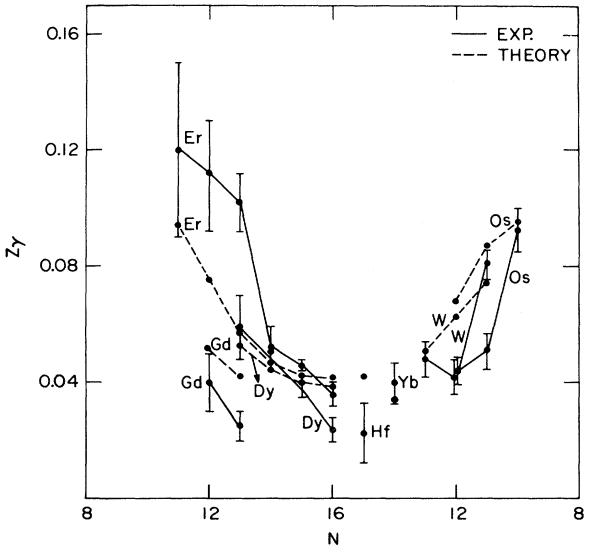

FIG. 4. Empirical and calculated Z_γ values plotted as a function of N. The points with error bars and the solid lines are taken from Fig. 1. The dashed lines connect the Z_γ values extracted from the IBA calculations.

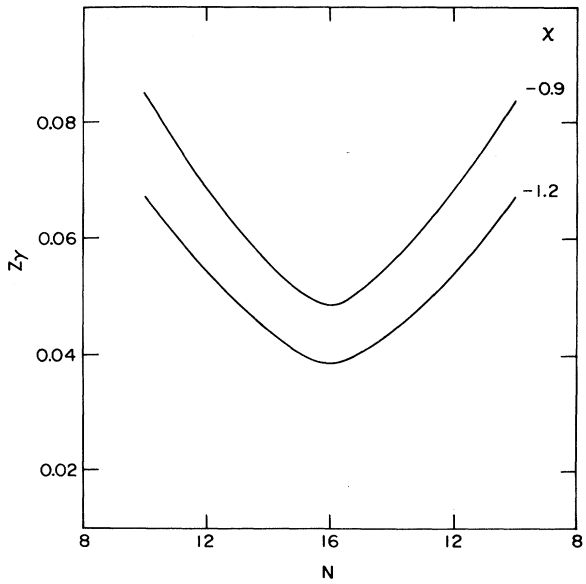

FIG. 5. Z_γ values extracted from IBA calculations for two values of Z_γ which conservatively encompass most well deformed rare earth nuclei.

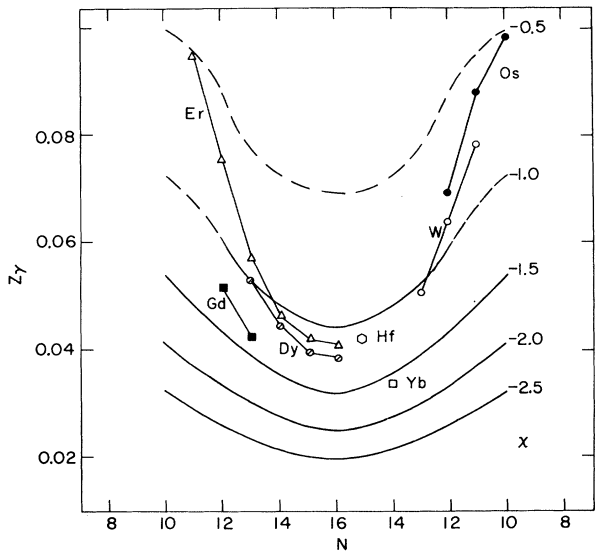

FIG. 6. Calculated Z_γ values as a function of N and χ. The lines show the systematic behavior of Z_γ as a function of N, for the constant χ values listed on the right. The dashed portions correspond to χ, N combinations for which the Mikhailov plots exhibit substantial curvature. These Z_γ values should be treated more qualitatively. The points are the calculated values for specific nuclei. They are plotted according to their boson number N and the χ values shown in Fig. 2.

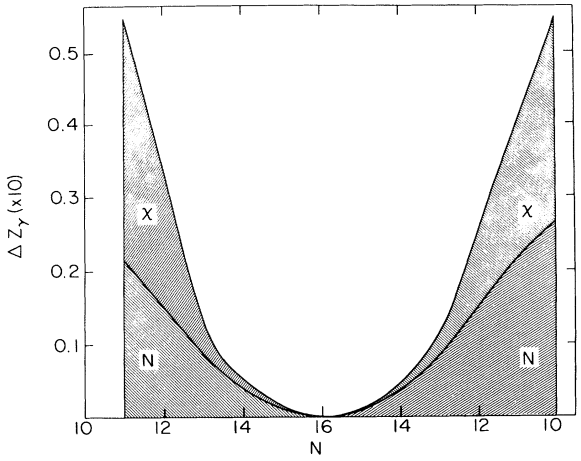

FIG. 7. The relative contributions to changes in Z_γ, relative to its value for $N=16$ and $\chi=-1.14$, due to changes in N and χ. The N contribution is obtained from a contour plot similar to Fig. 6 for $\chi=-1.14$. The χ contribution is obtained by utilizing a curve of χ values against N obtained by averaging the values in Fig. 2 (neglecting the anomalous Gd and Yb points) and then, for each N, taking the difference between Z_γ calculated for the appropriate χ value, and for $\chi=-1.14$.

by the effects of the steadily dropping N values, that lead to the large increase in γ-g mixing.

The respective roles of N and χ can be seen more quantitatively by drawing an average curve through the empirical χ values in Fig. 2 (neglecting for simplicity the anomalous Gd and Yb points) and then by plotting for each N the change in Z_γ, relative to its minimum value, for $\chi=-1.14$ and $N=16$, due to decreases in N and changes in χ. This is shown in Fig. 7 where, for any N, the height of each crosshatched area gives either the N or the χ effect. As pointed out above, it is clear that for the well deformed nuclei ($N\geq 12$) the boson number effects dominate, and give way to χ effects in the transitional regions.

C. Origin and interpretation of the $\gamma\rightarrow g$ transitions

It has been shown that the $\gamma\rightarrow g$ transitions in deformed nuclei empirically display a systematic pattern of deviations from the Alaga rules that is rather well reproduced in the IBA, largely as a result of variations in boson number N. The origin of these results in the IBA calculations can be understood in terms of the structure of the IBA Hamiltonian and the wave functions involved. Although the Hamiltonian is usually expressed in an SU(5) basis, this is not particularly convenient or illuminating for deformed nuclei. It is more useful to make a unitary transformation and deduce the effects of H in terms of matrix elements which admix SU(3) states. Figure 8 shows a plot, for 2^+ states, of the magnitude of some of the $\Delta K=0$ and 2 symmetry breaking matrix elements between SU(3) states as a function of χ. The most important feature, pointed out in an earlier study,[42,43] is the dominance of $\Delta K=0$ matrix elements. It will be shown that this is directly reflected in the resultant wave functions. As with the Hamiltonian, these wave functions are usually expressed in terms of SU(5) basis states. In deformed nuclei, however, they then become extremely complicated and hardly amenable to the recognition of simple regularities. An enormous simplification and ease of physical interpretation arises, however, if the IBA wave functions are reexpanded in an SU(3) basis. This approach has been discussed in Ref. 43 where, for example, the evolving structure of the low lying 2^+ states as a function of SU(3) symmetry breaking is readily apparent (see Fig. 1 of Ref. 43). In the context of the current formalism, which employs a consistent form of the quadrupole operator in H and $T(E2)$, Fig. 9 presents a similar decom-

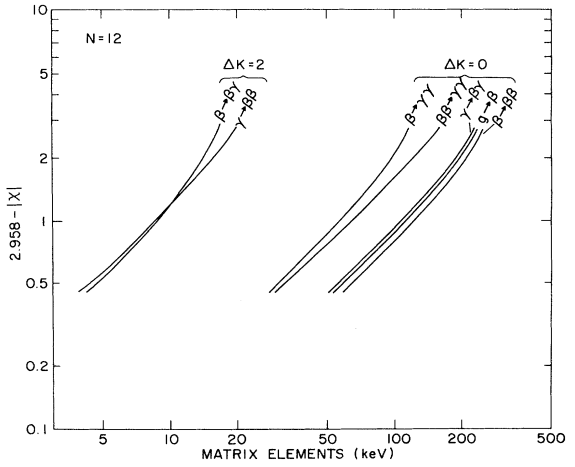

FIG. 8. The $\Delta K=0$ and 2 IBA matrix elements admixing SU(3) states, plotted as a function of χ for $N=12$.

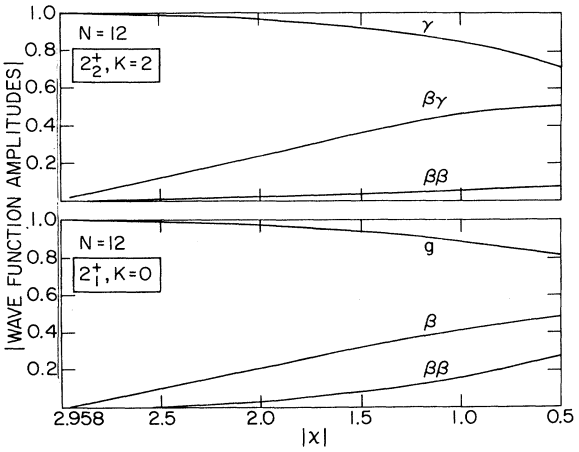

FIG. 9. Absolute values of the wave function amplitudes for the 2_γ^+ and 2_g^+ states expanded in the SU(3) basis as a function of χ.

position of the 2_g^+ and 2_γ^+ states, for $N=12$, in terms of the 2^+ states of the SU(3) g, β, $\beta\beta$, γ, and $\beta\gamma$ bands. The dominance of $\Delta K=0$ mixing in the Hamiltonian manifests itself in the principal SU(3) components appearing in the ground and γ bands, in particular in the large amplitude for the SU(3) β band in the ground band.

Since the decomposition of the wave function in terms of an SU(3) basis results in only a few (typically 2—5) important amplitudes, a corresponding simplification results in the structure of transition matrix elements. In general, any $E2$ matrix element can be written as

$$M(E2{:}I_i\rightarrow I_f)=\sum_{j,k}\alpha_{ij}\alpha_{fk}\langle\phi_k\,|\,E2\,|\,\phi_j\rangle\ , \tag{6}$$

where the basis states, ϕ, are those of SU(3). A matrix element such as $M(E2{:}\text{“}\gamma\text{”}\rightarrow\text{“}g\text{”})$ [where the quotation marks now refer to the actual IBA states, whereas, γ, g, etc., without quotation marks will refer to SU(3) basis states], will now have only a few appreciable terms, namely, only those where the expansion coefficients are sizable *and* where the elementary matrix element, $\langle\phi_k\,|\,E2\,|\,\phi_j\rangle$, connecting SU(3) basis states is large. It is important to point out that, in utilizing this approach, the elementary "SU(3)" matrix elements between SU(3) basis states must be calculated with an *E2 operator* involving the same χ value as in the actual calculation. Thus the so-called "elementary SU(3) matrix elements" are not strictly those of the SU(3) limit; in particular, *inter-representation* transitions, such as $\gamma\rightarrow g$, will be nonzero. Intra-representation transitions (such as $\beta\rightarrow\gamma$), however, are almost identical to their SU(3) values.

Thus, any $E2$ matrix element can be decomposed into its SU(3) amplitudes and several examples of this are provided in Fig. 4 of Ref. 43. It is also possible to utilize this decomposition technique to dissect a Mikhailov plot into its SU(3) constituents. Thus, for the $\gamma\rightarrow g$ transitions, the contribution from a given SU(3) transition is given by plotting

$$\alpha_{jI_\gamma}\alpha_{kI_g}\langle\phi_{jI_\gamma}\,|\,E2\,|\,\phi_{kI_g}\rangle/\sqrt{2}\langle I_\gamma 22-2\,|\,I_g 0\rangle \tag{7}$$

against the Mikhailov plot spin factor

$$I_g(I_g+1)-I_\gamma(I_\gamma+1)\ ,$$

keeping track of the appropriate sign of each component. Since the sum of terms on the right-hand side of Eq. (6) should add to the total matrix element on the left-hand side, the sum of the components of the Mikhailov plot should add to the full one. This allows one to easily identify those components which are dominant in determining the characteristic features of the full Mikhailov plot.

As an example, the upper part of Fig. 10 shows the major components of the Mikhailov plot for $N=16$ and $\chi=-1.5$. It can be verified that these components do account for most of the "$\gamma\rightarrow g$" matrix element by inspecting the lower part of the figure where the full Mikhailov plot, taken from the upper right box of Fig. 3, is compared with the sum of the components in the upper part. (The sum shown actually includes a few rather minor components omitted from the upper part simply to reduce clutter). Given this, it is evident that most of the *upslope* in the IBA Mikhaliov plot, that is, most of the deviations of "$\gamma\rightarrow g$" transitions from the Alaga rules, arises from that of two SU(3) components, the $\gamma\rightarrow g$ and the $\gamma\rightarrow\beta$ amplitudes. From the lower part of Fig. 10, it is evident that, of these, the $\gamma\rightarrow\beta$ component accounts for the major part of the slope, and moreover, that without these two components, the Mikhailov plot is essentially flat. It is interesting to note that the components which would contribute to the slope in a geometrical interpretation, namely the diagonal or intraband $g\rightarrow g$ and $\gamma\rightarrow\gamma$ amplitudes, are relatively unimportant.

Not only are the $\gamma\rightarrow g$ and $\gamma\rightarrow\beta$ amplitudes primarily responsible for most of the slope, but they also account for

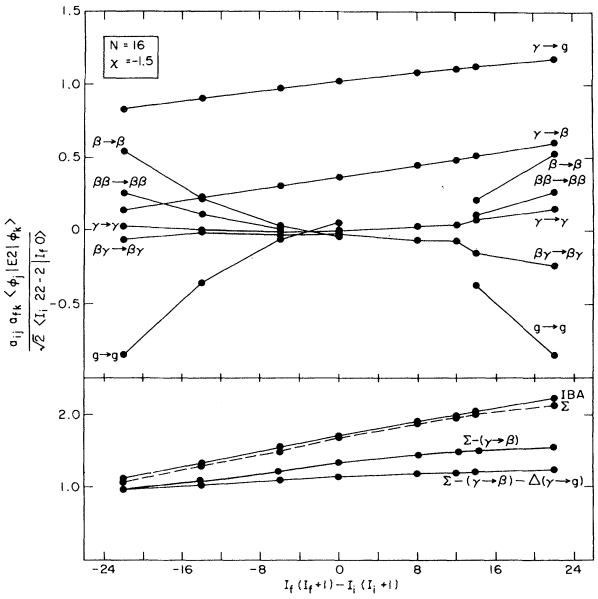

FIG. 10. Decomposition of the $\gamma\rightarrow g$ Mikhailov plot for $N=16$, $\chi=-1.5$ showing most of the major components of the calculated $\gamma\rightarrow g$ transitions. The lower part shows the IBA calculation (solid line), the sum of the major components (dashed line), most of which are included in the upper part, and this sum minus the $(\gamma\rightarrow\beta)$ and the rise $[\Delta(\gamma\rightarrow g)]$ in the $(\gamma\rightarrow g)$ components (solid lines).

the N dependence as well. Hence, a rather detailed but yet elementary understanding of the behavior of the IBA calculations of "$\gamma\rightarrow g$" transitions can be obtained by further study of these two constituent amplitudes.

This is easiest for the more important γ-β amplitude which arises from two aspects of the specific structure of the IBA in deformed nuclei, namely the large $\Delta K=0$ matrix elements that generate the SU(3) symmetry breaking and thereby admix substantial β amplitudes into the SU(3) ground band, and the allowed nature of the $\gamma\rightarrow\beta$ SU(3) transitions. Recalling that an allowed intra-representation transition, such as $\gamma\rightarrow\beta$, has almost no dependence on the values of χ chosen in the $E2$ operator, the role of finite N in such a transition can be assessed by inspecting its SU(3) behavior.

In the SU(3) limit of the IBA, the ground band is represented by the quantum numbers $(\lambda,\mu)=(2N,0)$, whereas the next representation is characterized by

$$(\lambda',\mu')=(\lambda-4,2)=(2N-4,2).$$

The $(2N-4,2)$ representation is comprised of two bands: a pure $K=0$ band, and a second band which is predominantly $K=2$ (γ band) with a small admixture of $K=0$. The SU(3) wave function of the predominantly $K=2$ band in the $(\lambda',\mu')=(2N-4,2)$ representation is then given by[2]

$$|(\lambda',\mu')\psi_2 I\rangle = X_0\,|(\lambda',\mu'),K=0,I\rangle + X_2\,|(\lambda',\mu'),K=2,I\rangle\ , \tag{8}$$

where $X_2\simeq 1$, and X_0 is given by

$$X_0=-\left[\frac{(I-1)(I)(I+1)(I+2)}{4(\lambda+2)(\lambda+3)(\lambda-I+2)(\lambda+I+3)}\right]^{1/2}. \tag{9}$$

Note that X_0 is effectively a γ-β mixing amplitude and that it has a strong N dependence (for $N\gg I$, $X_0\approx 1/\lambda^2\approx 1/N^2$). The slope, M_2, as mentioned earlier, in a Mikhailov formalism for $\Delta K=2$ mixing, is given by

$$M_2=(15/8\pi)^{1/2}eQ_0\epsilon_\gamma =(15/8\pi)^{1/2}eQ_0(N)X_0(N)/f'_\gamma(I)\ , \tag{10}$$

where the last expression uses Eqs. (8) and (9) and neglects the miniscule spin dependence in the denominator of X_0. Since the quadrupole moments of deformed nuclei are very closely proportional to N in the IBA, the N dependence of M_2, given by $Q_0(N)X_0(N)$, is well approximated simply by $1/N$. Thus, the basic structure of the γ and β bands in the SU(3) limit, which effectively involves a $\Delta K=2$ mixing, measured by X_0, *directly* leads to a strong N dependence in the $\gamma\rightarrow\beta$ contribution to "$\gamma\rightarrow g$" transitions.

To summarize, the γ-β contribution to the calculated "$\gamma\rightarrow g$" transitions arises from the large $\Delta K=0$ mixing characteristic of SU(3) symmetry breaking for typical deformed nuclei, which admixes large β components in the ground band, and from the group structure of the IBA which, contrary to the harmonic geometrical model, allows the component $\gamma\rightarrow\beta$ SU(3) transitions. The N *dependence* of the calculated γ-β contributions to the "$\gamma\rightarrow g$" transitions in turn stems from that of the γ-β *mixing inherent in the* SU(3) *limit.*

The origin of the slope and N dependence of the $\gamma\rightarrow g$ component of the "$\gamma\rightarrow g$" transition is more difficult to identify but also arises from finite N effects. In general, aside from the type of mixing arguments just discussed, any $E2$ matrix element in the IBA will also depend on those finite N effects which relate to the expectation values of the number of d bosons, $\langle n_d\rangle$, in the wave functions. Thus, *a priori,* it is not surprising that an IBA Mikhailov plot is not horizontal since $\langle n_d\rangle$ will be spin dependent and it will be different for different bands.

A measure of these effects in the present case is given by the normalized difference, Δn_d, in $\langle n_d(I)\rangle$ for the γ and g bands:

$$\Delta n_d(I_\gamma,I_g,N)=\frac{\langle n_d(I_\gamma)\rangle-\langle n_d(I_g)\rangle}{N-\langle n_d(I_g)\rangle}\ . \tag{11}$$

Values of Δn_d can be easily calculated from the SU(5) expansion of the wave functions. The calculations show that, for the same spin, $\langle n_d\rangle$ for the "γ" band is higher than for the "g" band. Thus finite dimensionality effects are not equal for the two bands. Moreover, the d boson number within a band increases with spin. Therefore, a spin *decreasing* $\gamma\rightarrow g$ transition such as a $6^+_\gamma\rightarrow 4^+_g$ transition will be much more affected by finite N than a spin *increasing* one such as $4^+_\gamma\rightarrow 6^+_g$. In fact, it turns out that a plot of Δn_d against the same abscissa as in the Mikhailov plot results in a straight line with finite slope and that the fractional change in this slope with decreasing N is directly proportional to the rate of change in the slope of the $\gamma\rightarrow g$ amplitude.

Very recently, the N dependence of these same $\gamma\rightarrow g$ transitions was calculated[44] analytically utilizing SU(3) wave functions and shown to be closely approximated by $1/\sqrt{N}$. Thus the N dependence of the "$\gamma\rightarrow g$" transitions results from the $1/N$ variation due to the $\gamma\rightarrow\beta$ component and the $1/\sqrt{N}$ variation arising from the $\gamma\rightarrow g$ component. Figure 11 shows the relative sizes of these two components, for $N=16$, by using the results of Fig. 10 and then, using this normalization, displays the changes in each component due to decreasing N. The solid line for the $\gamma\rightarrow\beta$ component is obtained from actual calculations. The dashed line is simply calculated from the variations in the calculated quadrupole moments and from the N dependence of the quantity [see Eq. (9)]

$$X'_0\equiv X_0(N)/f'_\gamma(I)\ ,$$

where the small I dependence remaining in X'_0 is neglected.

III. SUMMARY

A crucial test of collective models for deformed nuclei lies in their ability to correctly predict the deviations of inter-band transitions from the Alaga rules since such deviations reflect important nonrotational components in the wave functions. Empirically, the best studied of such transitions are those connecting γ and ground bands. The systematics of these deviations from the Alaga rules was extracted (in terms of Z_γ values) from the literature and shown to have a remarkably smooth, nearly parabolic, shape when plotted against boson number N. IBA calculations were shown to reproduce these systematics in an

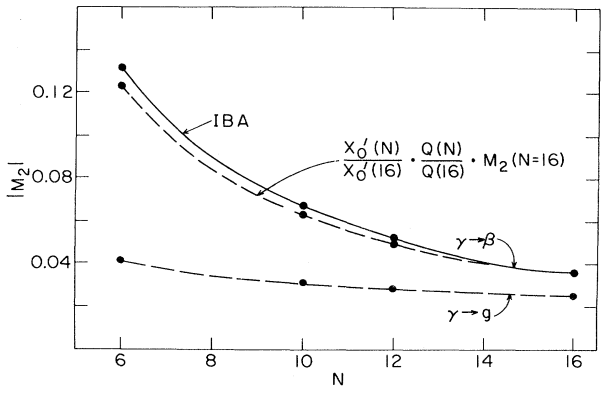

FIG. 11. Absolute value of the slope of the SU(3) $\gamma \rightarrow \beta$ and $\gamma \rightarrow g$ Mikhailov plots as a function N. The solid line for the $\gamma \rightarrow \beta$ slope is obtained from numerical calculations of these transitions. The dashed line for the $\gamma \rightarrow \beta$ transitions, which is normalized to the solid one at $N=16$, is obtained from the N dependence of the product $X_0' Q_0$, where $X_0' = X_0 / f_\gamma'(I)$ and where the very small remaining spin dependence of X_0' is neglected. The dashed line for the $\gamma \rightarrow g$ slope is obtained from Van Isacker's (Ref. 44) approximate expression, $M_2(\gamma \rightarrow g) \approx 1/\sqrt{N}$, and from the calculated value of the slope at $N=16$ obtained from Fig. 10.

extremely simple (consistent Q) formalism incorporating only one parameter, χ. This analysis permitted the isolation of χ and N effects and showed that, for the majority of well deformed nuclei, the principal determinant of the systematic behavior of "$\gamma \rightarrow g$" transitions is specifically the explicit N dependence in the IBA. Finally, it was shown that this N dependence arises primarily from the structure of the SU(3) wave functions, and from the predominantly $\Delta K = 0$ symmetry breaking which admixes SU(3) states to produce wave functions for realistic calculations. Specifically, it originates essentially from two sources, from the differences in average d boson number in the γ and g bands, and more importantly, from the dependence of the mixing of pure $K=0$ and 2 states on N to produce the analog of γ and β bands in the IBA. It is indeed because of such inherent *mixing* effects that the N dependence in "γ-g" transitions is much stronger than had been anticipated using the simple argument given in the Introduction.

It is important to assess the meaning of these results carefully, by distinguishing between *variations* in boson number and the *absolute value* of N. The present results demonstrate the fundamental importance of boson number variations in the IBA due to changes in mass. It does not establish, however, a specific value for N. Such a determination, if possible at all, must result from further studies, although recent work[45] on g factors near $Z=64$, $N=90$, in an IBA-2 context, has led to a very suggestive discrimination between two sets of proton boson numbers. Ultimately, this question is of substantial importance, both in assessing the role of intruder orbits in modifying the effective boson number applicable to a given nucleus, and since it represents the crucial foundation upon which any essential link with the underlying shell model basis must be built.

ACKNOWLEDGMENTS

We are grateful to Dr. A. Dieperink, Dr. J. Cizewski, Dr. F. Iachello, Dr. I. Talmi, Dr. A. Arima, and Dr. P. Van Isacker for fruitful discussions concerning the IBA treatment discussed herein and to L. L. Riedinger for numerous discussions of the band mixing phenomenon and formalism. This research was performed under contract DE-AC02-76CH00016 with the U.S. Department of Energy.

[1]A. Arima and F. Iachello, Ann. Phys. (N.Y.) 99, 253 (1976).
[2]A. Arima and F. Iachello, Ann. Phys (N.Y.) 111, 201 (1978).
[3]O. Scholten, F. Iachello, and A. Arima, Ann. Phys. (N.Y.) 115, 325 (1978).
[4]K. Kumar, *Progress in Particle and Nuclear Physics,* edited by Denys Wilkinson (Pergamon, New York, 1983), p. 233.
[5]H. Emling, P. Fuchs, E. Grosse, R. Kulessa, D. Schwalm, R. S. Simon, and H. J. Wollersheim, International Conference on Nuclear Behavior at High Angular Momentum, Strassbourg, France, Centre de Recherches Nucleaires Report, 1980.
[6]H. Ower, Th. W. Elze, J. Idzko, W. Stelzer, H. Emling, P. Fuchs, E. Grave, D. Schwalm, H. J. Wallersheim, N. Kaffrell, and N. Trautmann, J. Phys. (Paris) Suppl. No. 12, 1980 p. C10–102.
[7]H. P. Hellmeister, U. Kaup, J. Keinonen, K. P. Lieb, R. Rascher, R. Ballini, J. Delauney, and H. Dumont, Phys. Lett. 85B, 34 (1979); Nucl. Phys. A332, 241 (1979).
[8]D. D. Warner and R. F. Casten, Phys. Rev. Lett. 48, 1385 (1982).
[9]D. D. Warner, in the Proceedings of the Workshop on Boson Models, Drexel University, 1983 (to be published).
[10]R. Bijker and A. E. L. Dieperink, Phys. Rev. C 26, 2688 (1982).
[11]R. C. Greenwood, C. W. Reich, H. A. Baader, H. R. Koch, D. Breitig, O. W. B. Schult, B. Fogelburg, A. Backlin, W. Mampe, T. von Egidy, and K. Schreckenbach, Nucl. Phys. A304, 327 (1978).
[12]F. K. McGowan, Phys. Rev. C 24, 1805 (1981).
[13]W. F. Davidson, R. F. Casten, D. D. Warner, K. Schreckenbach, H. G. Borner, J. Simic, M. Stojanovic, M. Bogdanovic, S. Koicki, W. Gelletly, G. B. Orr, and M. L. Stelts, J. Phys. G 7, 455 (1981); 7, 843 (1981).
[14]R. F. Casten and D. D. Warner, in *Neutron Capture Gamma-ray Spectroscopy and Related Topics,* edited by T. von Egidy, F. Gonnewein, and B. Maier (Institute of Physics, London, 1982), Conf. Series No. 62, p. 28.
[15]D. D. Warner, R. F. Casten, and W. F. Davidson, Phys. Rev. C 24, 1713 (1981).
[16]L. L. Riedinger, Noah R. Johnson, and J. H. Hamilton, Phys. Rev. C 179, 1214 (1969).
[17]W. T. Milner, F. K. McGowan, R. L. Robinson, P. H. Stelson, and R. O. Sayer, Nucl. Phys. A177, 1 (1971).
[18]R. M. Ronningen, J. H. Hamilton, A. V. Ramayya, L. Varnell, G. Garcia-Bermudez, J. Lange, W. Laurens, L. L. Riedinger, R. L. Robinson, P. H. Stelson, and J. L. C. Ford, Jr., Phys. Rev. C 15, 1671 (1977).
[19]L. Varnell, J. H. Hamilton, and R. L. Robinson, Phys. Rev. C 3, 1265 (1971).

[20]A. Charvet, R. Duffait, A. Emsallem, and R. Chery, Nucl. Phys. A156, 276 (1970).
[21]R. G. Wilson, Phys. Rev. 178, 1949 (1969).
[22]D. G. Burke and B. Elbek, K. Dan. Vidensk. Selsk. Mat.-Fys. Medd. 36, No. 6 (1967).
[23]R. Hochel, P. J. Daly, and K. J. Hofsetter, Nucl. Phys. A211, 165 (1973).
[24]P. Aguer, C. F. Liang, J. Libert, P. Paris, A. Peghaire, A. Charvet, R. Duffait, and G. Marguier, Nucl. Phys. A249, 239 (1975).
[25]R. F. Casten, M. R. Macphail, W. R. Kane, D. Breitig, K. Schreckenbach, and J. Cizewski, Nucl. Phys. A316, 61 (1979).
[26]Y. Yoshizawa, B. Elbek, B. Herskind, and M. C. Olesen, Nucl. Phys. 73, 273 (1965).
[27]F. W. N. DeBoer, P. F. A. Goudsmit, B. J. Meijer, P. Koldewijn, J. Konijn, and R. Beetz, Nucl. Phys. A236, 349 (1974).
[28]F. W. N. DeBoer, P. F. A. Goudsmit, P. Koldewijn, and B. J. Meijer, Nucl. Phys A169, 577 (1971).
[29]P. Aguer, C. F. Liang, J. Libert, P. Paris, A. Peghaire, A. Charvet, R. Duffait, and G. Marguier, Nucl. Phys. A252, 293 (1975).
[30]S. W. Yates, P. J. Daly, Noah, R. Johnson, and N. K. Aras, Nucl. Phys. A204, 33 (1973).
[31]D. J. McMillan, R. C. Greenwood, C. W. Reich, and R. G. Helmer, Nucl. Phys. A223, 29 (1974).
[32]R. F. Casten, W. R. Kane, M. R. Macphail, J. A. Cizewski, A. Aprahamian, and D. Breitig (unpublished).
[33]R. Spanhoff, H. Postma, and M. J. Cantry, Phys. Rev. C 18, 493 (1978).
[34]S. W. Yates, J. C. Cunnane, and P. J. Daly, Phys. Rev. C 11, 2034 (1975).
[35]R. C. Thompson, J. S. Boyno, J. R. Huizenga, D. G. Burke, and Th. W. Elze, Nucl. Phys. A242, 1 (1975).
[36]R. F. Casten and J. A. Cizewski, Nucl. Phys. A309, 477 (1978).
[37]G. D. Dracoulis, C. Fahlander, and M. P. Fewell, Australian National University Report ANU-P/820, 1982.
[38]R. F. Casten, J. S. Greenberg, S. H. Sie, G. A. Burginyon, and D. A. Bromley, Phys. Rev. 187, 1532 (1969).
[39]D. L. Anderson and D. S. Brenner, Phys. Rev. C 18, 383 (1978).
[40]P. Hungerford, W. D. Hamilton, S. N. Scott, and D. D. Warner, J. Phys. G 6, 741 (1980).
[41]M. Fujioka, Nucl. Phys. A153, 337 (1970).
[42]R. F. Casten and D. D. Warner, see Ref. 4, p. 311.
[43]R. F. Casten and D. D. Warner, Phys. Rev. Lett. 48, 666 (1982).
[44]P. Van Isacker, Universidad Nacional Autonoma de Mexico report 1983.
[45]A. Wolf, Z. Berant, D. D. Warner, R. L. Gill, M. Shmid, R. E. Chrien, G. Peaslee, H. Yamamoto, John C. Hill, F. K. Wohn, C. Chung, and W. B. Walters, Phys. Lett. 123B, 165 (1983).